

DOI: <https://doi.org/10.24425/amm.2022.137496>A.R. KAMROSNI<sup>1\*</sup>, C.H. DEWI SURYANI<sup>1</sup>, A. AZLIZA<sup>1</sup>, A.B.A. MOHD. MUSTAFA<sup>1</sup>,  
M.S. MOHD. ARIF ANUAR<sup>1</sup>, M. NORSURIA<sup>1</sup>, V. CHOHPATTANA<sup>2</sup>, L. KACZMAREK<sup>3</sup>, B. JEŽ<sup>4</sup>, M. NABIAŁEK<sup>4</sup>

## MICROSTRUCTURAL STUDIES OF Ag/TiO<sub>2</sub> THIN FILM; EFFECT OF ANNEALING TEMPERATURE

Microstructures are an important link between materials processing and performance, and microstructure control is essential for any materials processing route where the microstructure plays a major role in determining the properties. In this work, silver-doped titanium dioxide (Ag/TiO<sub>2</sub>) thin film was prepared by the sol-gel method through the hydrolysis of titanium tetra-isopropoxide and silver nitrate solution. The sol was spin coated on ITO glass substrate to get uniform film followed by annealing process for 2 hours. The obtained films were annealed at different annealing temperatures in the range of 300°C-600°C in order to observe the effect on crystalline state, microstructures and optical properties of Ag/TiO<sub>2</sub> thin film. The thin films were characterized by X-Ray diffraction (XRD), scanning electron microscopy (SEM), and UV-Vis spectrophotometry. It is clearly seen, when the annealing temperature increases to 500°C, a peak at  $2\theta = 25.30^\circ$  can be seen which refers to the structure of TiO<sub>2</sub> tetragonal anatase. The structure of Ag/TiO<sub>2</sub> thin film become denser, linked together, porous and uniformly distributed on the surface and displays the highest cut-off wavelength value which is 396 nm with the lowest band gap value, which is 3.10 eV.

*Keywords:* Ag/TiO<sub>2</sub>; Annealing Temperature; Microstructure; Optical Properties; Thin Film

### 1. Introduction

Over the past few decades, continuous breakthroughs in the synthesis and modification of titanium dioxide which is known as titanium (IV) dioxide or titania (TiO<sub>2</sub>). TiO<sub>2</sub> is an important inorganic functional material with good physical and optical properties, which make it suitable for various applications. Recently, TiO<sub>2</sub> thin films are growing as one of the promising oxide materials due to the great chemical, physical, electrical and optical properties [1-4]. TiO<sub>2</sub> has been investigated by many researchers because of their numerous applications in various industries. Its high chemical stability, corrosion resistance and excellent optical transparency in the visible and near infrared regions, will give high refractive index which make it useful for optical devices [5].

Many studies on synthesis of TiO<sub>2</sub> and its thin films formed via conventional and advanced sol-gel methods have been reported. Previous investigations show that the properties of TiO<sub>2</sub> films appear to strongly effect on the process parameters and

precursors used in the processes. Therefore, most of researchers have used sol-gel method to synthesis TiO<sub>2</sub> thin films with different controlling parameters such as temperature and time of annealing, number of dipping or spinning, molar ratio of prepared solution, precursor solutions and the surfactant or dopant which were used in their research in order to get pure TiO<sub>2</sub> or to enhance the properties of TiO<sub>2</sub> for a certain application [6]. Microstructures are an important link between materials processing and performance, and microstructure control is essential for any materials processing route where the microstructure plays a major role in determining the properties [7]. In the application of photocatalysis devices, the synthesized microstructure strongly affected the performance of harvesting the sunlight.

One of the efficient ways of improving the properties of TiO<sub>2</sub> film is the addition of certain dopants. Many studies have been devoted to further improve the photocatalytic and antibacterial properties of TiO<sub>2</sub> thin films and the investigations suggest that those properties can be enhanced by doping with transition metal such as Ag [8], Fe<sup>3+</sup> [9], N [10] and Cu [11].

<sup>1</sup> UNIVERSITI MALAYSIA PERLIS, (UNIMAP), CENTER OF EXCELLENCE GEOPOLYMER & GREEN TECHNOLOGY (CEGEOGTECH), SCHOOL OF MATERIALS ENGINEERING, 02600 JALAN KANGAR- ARAU, PERLIS, MALAYSIA

<sup>2</sup> RAJAMANGALA UNIVERSITY OF TECHNOLOGY THANYABURI (RMUTT), FACULTY OF ENGINEERING, DEPARTMENT OF MATERIALS AND METALLURGICAL ENGINEERING, THAILAND

<sup>3</sup> LODZ UNIVERSITY OF TECHNOLOGY (TUL), INSTITUTE OF MATERIALS SCIENCE AND ENGINEERING, 1/15 STEFANOWSKIEGO STR., 90-924 LODZ, POLAND

<sup>4</sup> CZĘSTOCHOWA UNIVERSITY OF TECHNOLOGY, FACULTY OF PRODUCTION ENGINEERING AND MATERIALS TECHNOLOGY, DEPARTMENT OF PHYSICS, 19 ARMII KRAJOWEJ AV., 42-200 CZĘSTOCHOWA, POLAND

\* Corresponding author: kamrosni@unimap.edu.my



In this study, Ag/TiO<sub>2</sub> thin films were prepared via sol-gel spin-coating method using a specific ratio. The obtained thin films were annealed in various temperature to investigate the effect of annealing temperature on the crystalline state, microstructures and optical properties of Ag/TiO<sub>2</sub> thin film.

## 2. Materials and Methodology

Titanium (IV) isopropoxide 97% (TTIP) and silver nitrate (AgNO<sub>3</sub>) powder were obtained from Sigma Aldrich. Propan-2-ol was purchased from QReC Chemicals, while acetic acid (99.5%) was obtained from Daejung Reagent Chemicals. All the chemicals were analytical reagents and were used as received without further purification.

### 2.1. Preparations of the thin films

The Ti sol was prepared with specific ratio of xx. An amount of 0.5 ml TTIP precursor was dissolved in 20 ml of isopropanol and stirred continuously for 10 min at room temperature. A mixture of 0.1 ml water, 2.0 ml ethanol and 0.1 ml of 0.1 M AgNO<sub>3</sub> was added dropwise into the solution and stirring process was continued for another 10 min. Then a small aliquot of concentrated acetic acid with negligible dilution was added into the solution. The alkoxide solution was kept stirring at room temperature for hydrolysis reaction to occur for 5 min, resulting in the Ti-precursor sol.

The indium tin oxide (ITO) coated glasses (15 mm × 15 mm × 0.5 mm) were used as the substrates for the deposition of films. The substrates were degreased and cleaned with acetone for 30 min in an ultrasonic bath and thoroughly rinsed with water. Then, the substrates were dried at 90°C for 90 min in the oven and were kept in Petri dishes with lids for further use.

For making the Ag/TiO<sub>2</sub> thin film, one drop of Ti sol was deposited onto the pretreated ITO substrates by using a spin coating method that was conducted at 100 rpm for 10 s. After that, the spin speed was increased to 2000 rpm for 30 s in order to form a thin layer of film over the substrate. Then, the film was dried at 60°C for 10 minutes followed by the annealing process at 300°C for 2h in ambient atmosphere furnace. Three more thin film samples were prepared by using the similar method as described above and were annealed at 400°C, 500°C and 600°C, respectively. The heat-treated films were stored in Petri dishes with lid for further use.

### 2.2. Characterization of the thin films

The prepared Ag/TiO<sub>2</sub> thin films were characterized structurally through X-ray diffraction (XRD) which was measured in the range of 0°-80° using Cu Kα (λ = 1.5046). The morphology of the films was studied by using a field emission scanning electron microscopy (FESEM). The surface topography of the

films was examined by using an atomic force microscope (AFM) in a contact mode conditions. The optical properties of the film were characterized by using a UV-Vis spectroscopy.

## 3. Results and discussion

### 3.1. Phase analysis

Fig. 1 shows the XRD patterns of Ag/TiO<sub>2</sub> thin film at different annealing temperature. There are five peaks at 2θ = 21.5°, 30.57°, 35.40°, 51.04° and 60.70° corresponding to the peaks of ITO glass substrate. No trace of TiO<sub>2</sub> peaks can be observed for the non-annealing film and the films that were annealed at 300°C and 400°C, respectively, which might indicate that TiO<sub>2</sub> is still in an amorphous phase. In this case, the thermal energy supplied by those annealing temperature range is not sufficient for the crystallization process to occur [12]. When the annealing temperature were increased up to 500°C, it can be clearly seen a (101) anatase peak at 2θ = 25.30° (JCPDS PDF-021-1272). The intensity of this peak becomes stronger as the annealing temperature was increased to 600°C.

Based on the XRD data, the FWHM values were decreasing and narrowing, indicating an increase in particle size as the annealing temperature increased [13]. For confirmation,

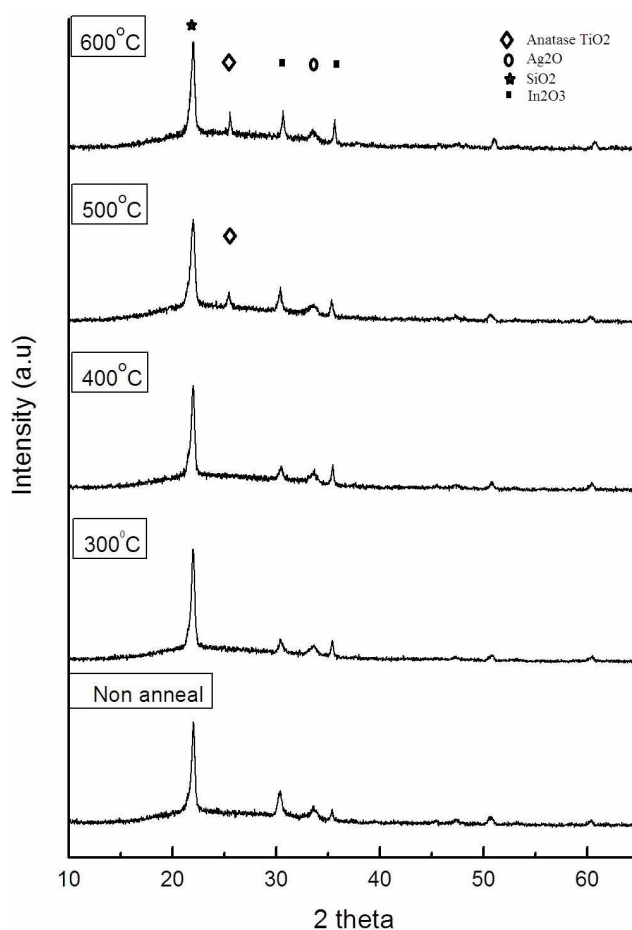


Fig. 1. XRD patterns of Ag/TiO<sub>2</sub> thin films with different annealing temperatures

the crystallite size of the TiO<sub>2</sub> films were estimated by using the Scherrer equation as follows:

$$D = (K \lambda) / (\beta \cos \theta) \quad (1)$$

where  $K = 0.9$  is the Scherrer coefficient,  $\lambda = 1.540598 \text{ \AA}$  is the Cu K $\alpha$  radiation wavelength,  $\beta$  is the full width at half maximum (FWHM) of the diffraction peak, and  $\theta$  is the diffraction angle of the diffraction peak. The crystallite size of the anatase film that was annealed at 500°C was 40.4 nm. The crystallite size grew about 13.8% (46.0 nm) when the annealing temperature was increased to 600°C. This finding is supported by previous studied by [12,14] which also reported that the size of crystallite increases as the temperature of the annealing process increases.

### 3.2. Surface Morphology and Surface Roughness

Scanning electron microscope (SEM) was utilized to observe the surface morphology of Ag/TiO<sub>2</sub> thin films that were heat-treated with different annealing temperatures. Fig. 2 shows the SEM images of obtained thin films with non-annealing and various annealing temperature. For the non-annealed film (Fig. 2(a)), the film structure was porous and uniformly distributed throughout the substrate, with non-homogenous shapes. As the thin films were annealed at 300°C and 400°C, a chain-like structure could be detected, that linked the structures together, as shown in Fig. 2(b) and Fig. 2(c). During the heat treatment up to 200°C, most organic solvents were burned, leading to the formation of the porous and amorphous structure of the TiO<sub>2</sub> film [15]. When the thin film was annealed at 500°C, the structure become denser, linked together, porous and uniformly distributed on the surface as shown in Fig. 2(d). At this stage, the TiO<sub>2</sub> sol had enough energy to crystallize into the anatase phase as proved by the XRD pattern in Fig. 1. When the annealing was increased to 600°C, as seen in Fig. 2(e), the thin film was in porous structure with a wider distance between the linkage of the TiO<sub>2</sub>.

The surface morphology and surface roughness of the produced films at different annealing temperatures were observed through the AFM analysis. Fig. 3 shows the top view and angle view of the obtained Ag/TiO<sub>2</sub> thin film. In AFM analysis, root mean square (RMS) is a parameter that is commonly used for characterization of the surface roughness [16]. TABLE 1 shows surface roughness value of thin film produced at different annealing temperatures.

As observed in Fig. 3(a), non-annealed thin film exhibits a rough structure uniformly distributed throughout the substrate, but the crystal grain cannot be seen clearly. This indicates that the thin film particle is in an amorphous phase with surface roughness of 1.81 nm. According to Mosquera et al. (2015), rough structure and the absence of a fine atomic terrace indicates that the sample deposited as amorphous [17]. After annealing process at 300°C, the obtained thin film structure is not much different from the non-annealed thin film but the surface roughness increases to 4.36 nm, as shown in Fig. 3(b). There is also agglomeration of particles which display a non-uniform particle distribution.

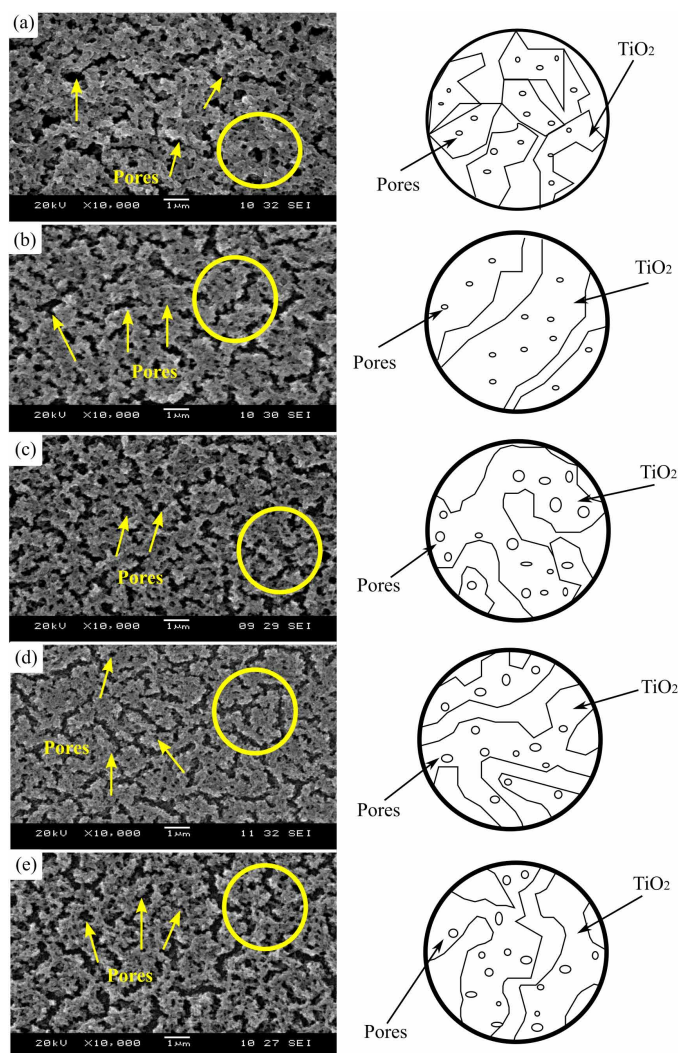


Fig. 2. SEM micrograph of Ag/TiO<sub>2</sub> thin film with different annealing temperature, (a) non-annealing, (b) 300°C, (c) 400°C, (d) 500°C and (e) 600°C

At 400°C annealing temperature (Fig. 3(c)), the Ag/TiO<sub>2</sub> thin film shows a rough and porous structure. For a thin film that heated over 200°C, most of the organic solvent were decomposed, thus forming a porous and amorphous TiO<sub>2</sub> thin film [15]. Increasing of annealing temperature can cause the grain to agglomerate thus makes the surface rugged with surface roughness of 9.68 nm. This uneven shape of nanoparticles was caused by low temperature and not enough kinetic energy to induce the crystallization of the particles [12].

TABLE 1

Surface roughness value of thin film produce at different annealing temperatures

Ag/TiO <sub>2</sub> Thin Film	Annealing Temperature	Root Mean Square (RMS)
(a)	Non-Anneal	1.81 nm
(b)	300°C	4.36 nm
(c)	400°C	9.68 nm
(d)	500°C	1.86 nm
(e)	°C	3.92 nm

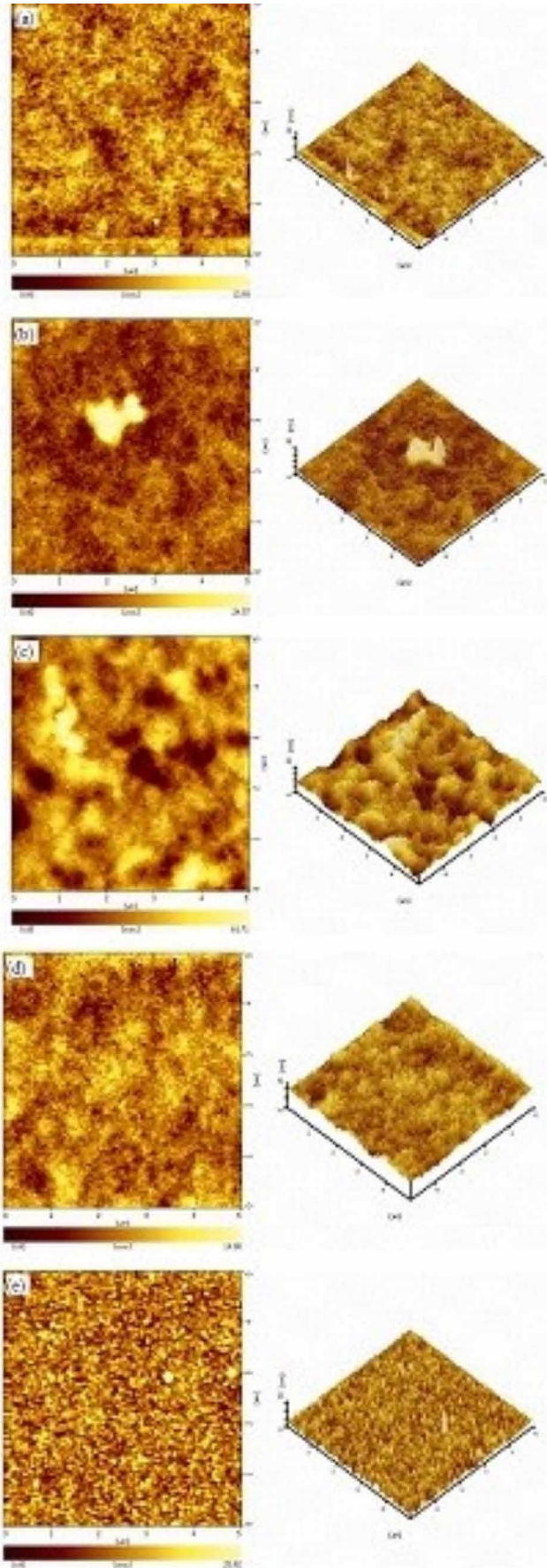


Fig. 3. Surface morphology of Ag/TiO<sub>2</sub> thin films at different annealing temperature, (a) non-annealing, (b) 300°C, (c) 400°C, (d) 500°C and (e) 600°C

At 500°C annealing temperature, the thin film shows a fine structure with small grain size, as seen in Figure 3(d). At this state, TiO<sub>2</sub> particles have enough energy to crystallize into anatase phase, as proved by the XRD analysis. When the annealing temperature was increased to 600°C, the grain structure of the thin film became bigger that resulting in a rough surface with surface roughness of 3.92 nm. Increasing the annealing temperature could increase the grain size of the TiO<sub>2</sub> particles and resulting on the increasing of surface roughness [18] due to microstructure phase transformation [17].

### 3.3. Optical properties

Optical properties of Ag/TiO<sub>2</sub> thin film with 0.1 M concentration of Ag was studied to observed the effect of different annealing temperatures using UV-Vis spectrophotometer. Fig. 4 shows the light absorption of Ag/TiO<sub>2</sub> thin film at different annealing temperature in the spectrum range of 300 nm to 500 nm. The absorption edge shifts as the annealing temperature increase. Non-annealed Ag/TiO<sub>2</sub> thin film exhibits low absorption which is 0.57 (arbitrary unit) at wavelength 375 nm and increase to 1.07 (arbitrary unit) when annealed at temperature of 300°C. Ag/TiO<sub>2</sub> thin film with 500°C annealing temperature shows the highest absorption at 375 nm wavelength which is 1.17 (arbitrary unit). Value of cut-off wavelength increase as the annealing temperature increase.

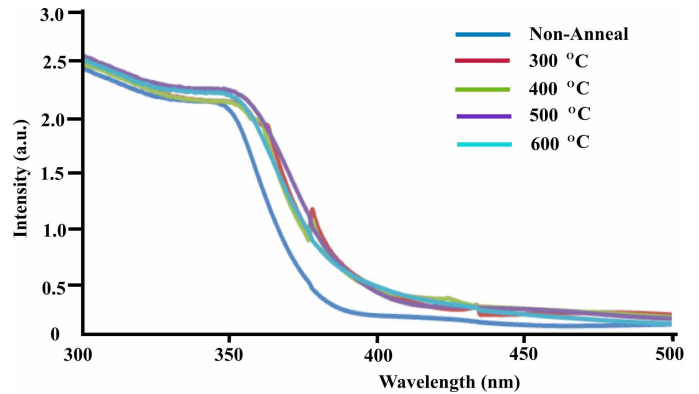


Fig. 4. Absorption curve of Ag/TiO<sub>2</sub> thin film at different annealing temperature in the spectrum range of 300 nm to 500 nm

TABLE 2 present cut-off wavelength value and band gap value for Ag/TiO<sub>2</sub> thin film annealed at different temperature. Overall, the cut-off wavelength for all produced thin films are in the spectrum range exceeded 369 nm, which are higher than anatase TiO<sub>2</sub> cut-off wavelength values [19].

Cut-off wavelength values increase when the annealing temperature increased. In contrast, as the annealing temperature increase, the band gap value decreases. Ag/TiO<sub>2</sub> thin film that have been annealed at 500°C displays the highest cut-off wavelength value which is 396 nm with the lowest band gap value, which is 3.13 eV. This situation is due to the increasing crystal size from agglomeration at higher temperature [20]. Nevertheless, Ag/TiO<sub>2</sub> thin film at highest annealing temperature, 600°C

TABLE 2  
 Band gap value for Ag/TiO<sub>2</sub> thin film with different annealing temperature

Annealing temperature (°C)	Cut-off wavelength (nm)	Band gap (eV)
Non-annealed	379	3.27
300	382	3.45
400	388	3.19
500	396	3.10
600	390	3.18

shows less cut-off wavelength value which is 390 nm while the band gap value is 3.18 eV.

#### 4. Conclusion

In this work, the Ag/TiO<sub>2</sub> was deposited onto glass substrate via sol-gel spin coating method. The deposited films were annealed at 300-600°C. The effect of different annealing temperatures on the formation of Ag/TiO<sub>2</sub> thin films were successfully observed. The results show;

- The XRD pattern clearly shows the anatase phase when the annealing temperature increased to 500°C and 600°C.
- The SEM micrograph showed that for the non-annealing film, the film structure was porous and uniformly distributed throughout the substrate, with non-homogenous shapes. When the thin film was annealed at 500°C, the structure become denser, linked together, porous and uniformly distributed on the surface.
- Surface topographical profile shows that non-anneal thin film exhibits a rough structure uniformly distributed throughout the substrate, but the crystal grain cannot be seen clearly. This shows that this thin film particle is in amorphous phase with surface roughness of 1.81. At 500°C annealing temperature, the thin film shows a fine structure with small grain size. At this state, TiO<sub>2</sub> particles had enough energy to crystallize into anatase phase, as proved by the XRD analysis. When the annealing temperature increases to 600°C, the grain structure of the thin film becomes bigger and resulting in a rough surface with surface roughness of 3.92.
- The light absorption edge shifts as the annealing temperature increase. Ag/TiO<sub>2</sub> thin film that have been annealed at 500°C displays the highest cut-off wavelength value which is 396 nm with the lowest band gap value, which is 3.13 eV.

#### Acknowledgements

The author would like to acknowledge the support from the Fundamental Research Grant Scheme (FRGS) under a grant number of FRGS/1/2017/TK07/UNIMAP/02/6 from the Ministry of Education Malaysia and under grant number 9002-0082 from Tin Board Industry Grant. The authors wish to thank the Center of Excellence Geopolymer & Green Technology

(CEGeoGTech), School of Materials, Engineering, Universiti Malaysia Perlis, UniMAP for their partial support.

#### REFERENCES

- [1] M.T. Norman, M.A. Ashraf, A. Ali, *Environ. Sci. Pollut. Res.* **26**, 3262-3291 (2019).
- [2] A. Marzec, M. Radecka, W. Maziarz, A. Kusior, Z. Pedzich, *Journal of the European Ceramic Society* **36**, 2981 (2016).
- [3] A. Lewkowicz, A. Synak, B. Grobelna, P. Bojarski, R. Bogdanowicz, J. Karczewski, K. Szczodrowski, M. Behrendt, *Optical Materials* **36**, 1739 (2014).
- [4] D.S.C Halin, K.A. Razak, M.A.A.M. Salleh, M.I.I. Ramli, M.A.A.B. Abdullah, A.W. Azhari, K. Nogita, H. Yasuda, M. Nabialek, J.J. Wyslocki, *Magnetochemistry* **7** (1), 14 (2021).
- [5] A. Elfanaoui, E. Elhamri, L. Boukaddat, A. Ihlal, K. Bouabid, L. Laanab, A. Taleb, X. Portier, *Int. Journal of Hydrogen Energy* **36**, 4130 (2011).
- [6] K.A. Razak, D.S.C. Halin, M.M.A. Abdullah, M.A.A.M. Salleh, N. Mahmed, N.S. Danial, *Solid State Phenomena* **280**, 26-30 (2018).
- [7] J. Borges, M.S. Rodrigues, C. Lopes, D. Costa, F.M. Couto, T. Kubart, B. Martins, N. Duarte, J.P. Dias, A. Cavaleiro, T. Polcar, F. Macedo, F. Vaz, *Applied Surface Science* **358**, Part B, 595-604 (2015).
- [8] K. Ubolchonlakate, L. Sikong, T. Tontai, *J. Nanosci. Nanotechnol.* **10**, 1-4 (2010).
- [9] S. Boonyod, W. Sutthisripok, L. Sikong, *Adv. Mater. Res.* **214**, 197-201 (2011).
- [10] X. Mingyang, Z. Jinlong, C. Feng, *Appl. Catal. B Environ.* **89**, 563-9 (2009).
- [11] R. Vidhya, M. Sankareswari, K. Neyvasagam, *Int. Journal of Technical Research and Applications Special Issue* **37**, 42-46 (February, 2016).
- [12] A.S. Bakri, M.Z. Sahdan, F. Adriyanto, N.A. Raship, N.D.M. Said, S.A. Abdullah, M.S. Rahim, *AIP Conference Proceedings* **1788**, 030030 (2017). DOI: <https://doi.org/10.1063/1.4968283>
- [13] S. Saalinraj, K.C. Ajithprasad, *Materials Today Proceedings* **4**, 4372-4379 (2017).
- [14] Y. Rambabu, Manu Jaiswal, Somnath C. Roy, *Catalysis Today* **278**, 255-261 (2016).
- [15] B. Zhang, C. Xu, G. Xu, S. Tan, J. Zhang, *Optical Materials* **89**, 191-196 (2019). DOI: <https://doi.org/10.1016/j.optmat.2019.01.034>
- [16] R. Mechiakh, N. Ben Sedrine, J. Ben Naceur, R. Chtourou, *Surf. Coatings Technol.* **206** (2-3), 243-249 (2011).
- [17] A.A. Mosquera, J.M. Albella, V. Navarro, D. Bhattacharyya, J.L. Endrino, *Scientific Reports* **6**, 32171 (2015).
- [18] K. Sahbeni, I. Sta, M. Jlassi, M. Kandyla, M. Hajji, M. Kompitsas, W. Dimassi, *J. Phys. Chem. Biophys.* **7**, 257 (2017)
- [19] Y. Wu, Geis-Gerstorfer, L. Scheideler, F. Rupp, *Biofouling* **32** (5), 583-95 (2016). DOI: <https://doi.org/10.1080/08927014.2016.1170118>.
- [20] A. Lahmar, A. Benchaabane, M. Aderdour, A. Zeinert, M. Es-Souni, *Appl. Phys. A* **122**, 137 (2016)